UDC UDC 661.883.2/888.1:621.793.7

**J. C. Caicedo[1,*], W. F. Piedrahita[1], W. Aperador[2]**

[1]Tribology Powder Metallurgy and Processing of Recycled Solids Research Group, Universidad del Valle

[2]Department of Engineering, Universidad Militar Nueva Granada, Bogotá, Colombia

**julio.cesar.caicedo@correounivalle.edu.co*

# Physical properties comparison between hafnium and vanadium carbonitride coatings

*Hf–C–N and V–C–N coatings were deposited onto silicon (100) and AISI 8620 steel substrates by reactive r.f. magnetron co-sputtering from hafnium, vanadium and carbon targets in a reactive nitrogen atmosphere, with a negative bias voltage of –50 V. The effect of the Hf and V elements on the crystalline structure, chemical composition, and mechanical properties was observed via X-ray diffraction, X-ray photoelectron spectroscopy, Fourier transform infrared spectroscopy, computational simulation, atomic force microscopy, scanning electron microscopy, nanoindentation, pin on disk and scratch test techniques. The results show that the samples present constant stoichiometric ratio, exhibiting structural characteristics very similar to simulated structures. The changes in the mechanical properties by substituting the element Hf by V could increase the hardness from 22 to 24 GPa and the elastic modulus from 235 to 246 GPa. For tribological properties, changes from 0.49 to 0.42 for the friction coefficient and from 21 to 25 N for the critical load were found. So the influence of deposition conditions on the structure and properties of coatings was associated to differences in the content of hafnium and vanadium in ternary coatings. Therefore, the Hf–C–N and V–C–N coatings can be used as future hard coating materials.*

***Keywords**: Magnetron sputtering, metal carbon-nitrides, HfCN, VCN, mechanical properties.*

## INTRODUCTION

Nitrogen and carbon can form several compounds with most elements, the difference between the electronegativity of nitrogen or carbon and the other element that forms the carbonitride, the size of the respective atoms, and the electronic binding characteristics of these atoms are fundamental characteristics to form the ternary compound. Refractory nitrides are very similar to refractory carbides due to the good physical and chemical properties they have, for example their high melting point, good chemical stability, high hardness, wear resistance, among others. Refractory carbonitrides are very important in many industries due to their main applications in cutting tools, semiconductors and other mechanical components that require high resistance to wear, corrosion and prolongation of their service life [1–4].

The transition metal carbonitrides based on Hafnium and Vanadium are interstitial carbonitrides that have melting points above 2500 °C, obtaining several characteristics that classify them as important for the industry; they have complex electronic bound systems which includes ionic, covalent and metallic bounds, they

have mainly non-stoichiometric phases, like ceramics, they have high hardness and toughness, and as well as metals, they have high thermal and electrical conductivity [5]. In interstitial carbonitrides the difference in electronegativity between carbon, nitrogen and transition metals is large, as well as its atomic size. This allows the nitrogen and carbon atoms to be located more easily in the interstices of the metal crystalline structure, therefore, these carbonitrides generally have metal bonds with some covalent and ionic bonds. These characteristics give it different properties such as high electrical and thermal conductivity, high melting points, high hardness, and producing a chemical stability (chemically inert) [6].

The crystalline structure, phase analysis, hardness, internal stresses, adhesion, and wear resistance results, show that the properties of the Hf–CN and VCN coatings were less influenced by the deposition process than the HfN and VN coatings in relation to the deposition parameters selected. The behaviors of Hf–C–N and V–C–N carbonitrides have shown tribological applications in mechanical devices. It was also evidenced that the fundamental properties of these coatings are in many cases similar. For the application of these coatings in mechanical tools there are two interesting facts: For tribological application, coatings with a minimum thickness in the order of microns can be produced in a shorter time because the process is so sensitive to the deposition parameters, for example, the deposition rate and the bias voltage. In this sense, the physical and electrochemical properties are easier to reproduce; likewise, the studies reported in literature on the direct correlation among the deposition parameters, the internal stress and the physical properties of the hafnium and vanadium carbonitrides, promise to present the best mechanical, tribological and electrochemical properties [3, 7–9]. Regardless of this, and to the best of our knowledge, no previous reports are available on comparison of the physical properties for Hf–C–N and V–C–N coatings. Taking into account the aforementioned, the synergy between experimental conditions and physical properties (hardness) of 8620 steel substrate coated with Hf–C–N and V–C–N has yet to be thoroughly studied. In this work, Hf–C–N and V–C–N coatings with thickness in the range of ~1.5 μm were deposited on Si (100) and industrial steel substrates, seeking to study the structural and chemical evolution, crystallography simulation, as well as the comparison of the mechanical and tribological properties between both coatings. Thus, potential technological applications could be expected for the metal and mechanical industries.

## EXPERIMENTAL DETAILS

Hafnium carbon nitride and Vanadium carbon nitride coatings were deposited on silicon (001) and AISI 8620 steel substrates by reactive r.f. magnetron co-sputtering using a multi-target Intercovamex$^{TM}$ V4 facility at a base pressure of $10^{-4}$ Pa. Deposition was conducted by using Hf, V (99.99 % purity) and C (99.99 % purity) targets, each with a 10-cm diameter; a working pressure of 0.12 Pa in a mixture of 50 sccm (Ar) and 16 sccm ($N_2$) at 300 °C. The applied r.f. power density on the Hf, V and C targets was 5.0 W/m$^2$ per target. Distance between the targets and substrates was about 7 cm. Prior to deposition, the silicon and steel substrates were cleaned via r.f. negative bias of 200 V in 1.2 Pa of pure Ar atmosphere for 20 min. The control of Hf, V, C and N elements into the Hf–C–N and V–C–N coatings was carried out with the applied power to Hf, V and C targets and gas relation of Ar/$N_2$ (70 %/30 %). The coatings were deposited under circular rotation (60 rpm) by applying r.f. negative bias voltages of –50 V, to substrates with 2-h of deposition time. The Hf–C–N and V–C–N coatings' crystallography structure was obtained through X-ray diffraction (PANalytical X'Pert Pro$^{TM}$)

with a Cu$K\alpha$ radiation source (1.54051 Å). X-ray photoelectron spectroscopy (XPS) analyses were performed on a SAGE HR100 (SPECS$^{TM}$) with a monochromatic source (Mg$K\alpha$ 1253.6 eV) after sample surface etching to remove contamination. The chemical composition of the samples was obtained from the areas of the peaks by using the CasaXPS V2.3.15dev87$^{TM}$ software. Fourier Transform Infrared Spectroscopy (FTIR) was performed with Shimadzu 8000$^{TM}$ equipment, using a ceramic-type Nerst source. This assay was performed to find the active vibration modes in the infrared, corresponding to Hf–C–N and V–C–N bonds present in coatings deposited on silicon (100) substrates in transmittance mode. Atomic Force Microscopy (AFM) with a Multimode configuration was used for a quantitative study of the surface morphology (grain size and roughness) in HfCN and VCN coatings using an AFM Asylum Research MFP-3D®. All images were acquired in tapping mode and calculated by a Scanning Probe Image Processor (SPIP®) with their respective statistical analysis. For crystallography simulations of Hf–C–N and V–C–N materials the CaRIne crystallography 3.1 software was used. The software performs crystallographic simulations by taking into account the crystallographic structure, the spatial group and the atomic occupation sites (stoichiometric material). Coating thickness and cross-section morphology were determined by scanning electron microscopy (SEM) (JEOL JSM-6490LV$^{TM}$). Mechanical analyses were performed via nano-indentations by using an Ubi1-Hysitron$^{TM}$ device and a diamond Berkovich tip at variable loads. From these measurements, load–penetration depth curves of the coatings were obtained. Furthermore, hardness and elastic modulus values were determined from the load–displacement curves. Errors were determined as the standard deviation from at least 10 different measurements in different points of the samples. Tribological characterization was done by means of Microtest, MT 400-98 tribometer, using a 6-mm diameter 100Cr6 steel ball as pattern slide. The applied load was 0.5 N with a total 1000-m running length of pin-on disk test. Adherence of the layers was studied by using a Scratch Test Microtest MTR2 system; the parameters were a 6-mm scratch length and a raising load of 0–40 N.

## RESULTS AND DISCUSSION

### X-ray diffraction analysis

X-ray diffraction patterns of Hf–C–N and V–C–N coatings deposited on silicon substrates are shown in Fig. 1 for carbon nitride coatings deposited with different metal transition (Hf and V). For the HfCN coating, Fig. 1, *a* shows the analytical reference files; JCPDF 00-00-06-0516 and JCPDF 00-00-06-0510 of ICCD charts are shown for HfN and HfC, respectively. For the VCN coating Fig. 1, *b* presents the analytical reference files and JCPDF 00-035-0768 and JCPDF 01-073-0476 of ICCD of ICCD charts corresponding to VN and VC, respectively.

The diffraction patterns (see Fig. 1) show the Hf–C–N and V–C–N layers with face-centered cubic (FCC) NaCl F-type crystal structure [9–11]. The Hf–C–N and V–C–N coatings grow, similar to other ternary coatings such as TiCN [12, 13]; therefore, the crystals structures of Hf–C–N and V–C–N are associated to a substitution mechanism where the nitrogen atoms replace carbon atoms, resulting in an ordered Hf and V system and a disordered C–N system within the FCC-type NaCl structure, where Hf and V are located at the Wyckoff 4a site, while the carbon and nitrogen atoms randomly occupy the Wyckoff 4b site [14–16]. By considering said substitution mechanism, it is possible to conclude that the Hf–C–N and V–C–N systems obey a conjugated complex based on a substitutional solid solution, which considers Hf–C–N and V–C–N materials to come from an ideal

mixture between HfN and HfC for Hf–C–N and VN and VC for V–C–N coatings grown from the previous two materials respectively, these coating share the same crystal system FCC-type NaCl and space group 225-*Fm*-3*m* (see Fig. 1).

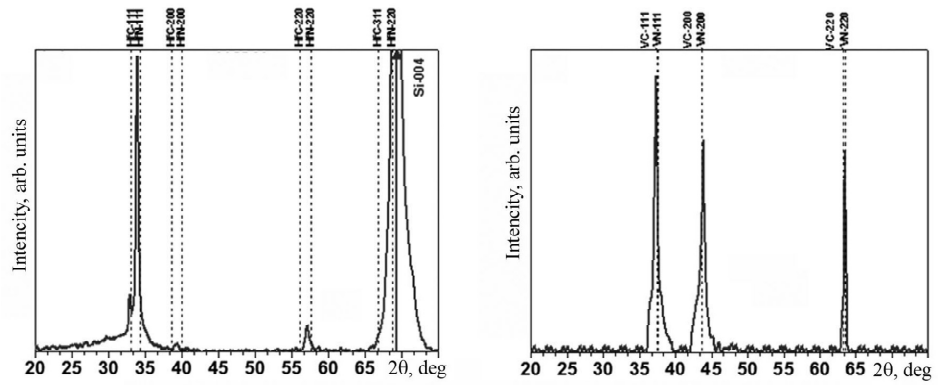


*a* *b*

Fig. 1. Diffraction patterns of Hf–C–N (*a*) and V–C–N (*b*) coatings deposited on Si (100) substrates with a negative bias voltage of –50 V. Dotted lines indicate the position of the peaks obtained from international (JCPDF) index files of HfN, HfC, VN and VC.

## X-ray photoelectron spectroscopy (XPS)

X-ray Photoelectron Spectroscopy (XPS) technique was used to obtain information about the atomic bonds and stoichiometry present in the Hf–C–N and V–C–N coatings. Figure 2 shows the complete survey spectra for both coatings. The Si2s (150.50 eV) and $Si2p_{3/2}$ (99.27 eV) peaks correspond to the silicon substrate. The remaining spectra show considerable intensity peaks located at 529.75, 395.25, 285.25, 16.25 and 514.40 eV, corresponding to the bonding energies of O1s, N1s, C1s, $Hf4f_{7/2}$ and V2p, respectively; significant oxygen peaks are present, probably due to sample contamination. It is evident that the binding energies for the C1s and N1s in Hf–C–N and V–C–N are slightly higher than HfC and HfN energies for HfCN and higher than VC and VN energies for VCN, consistent with results reported in specialized literature [17–20]. Additionally, it is possible to analyze the changes in binding energy of HfC and HfN for Hf–C–N coatings and VC and VN for V–C–N coatings, revealing the formation of two ternary compounds, Hf(C–N) and V(C–N), from binary materials.

The high-resolution spectra for C1s, N1s, Hf4f and V2p signals from Hf–C–N and V–C–N coatings grown under –50 V bias were taken from the inspection of the survey spectrum associated to Hf–C–N and V–C–N coatings (Fig. 3). The corresponding C1s peak in the high-resolution spectra is observed in Fig 3, *a*, this peak can be adjusted by three Gaussian functions; the respective deconvolution is obtained from three curves comprising the C1s signal, which means three binding energies, 281.46, 285.02, and 287.56 eV in C1s, assigned to C–Hf, C–C, and C–N bonds, respectively, agreeing with [19–21] for Hf–C–N materials. For the V–C–N system the C1s peak in the high-resolution spectra was also observed (see Fig 3, *a*), which can be adjusted by three Gaussian functions; the respective deconvolution is obtained from three curves comprising the C1s signal, which means three binding energies, 286.7, 285.0, and 282.8 eV in C1s, assigned to C=N, C–C, and C–V bonds, respectively [10–15, 22–28]. The interaction of elementary signals with the resulting binding energies represent a reaction between hafnium, carbon and nitrogen to form the ternary Hf–C–N compound, showing a stoichiometry of

$Hf_{57}C_{20}N_{23,}$ and the reaction between vanadium, carbon and nitrogen to form the ternary V–C–N material exhibiting the $V_{47}C_{21}N_{32}$ stoichiometry.

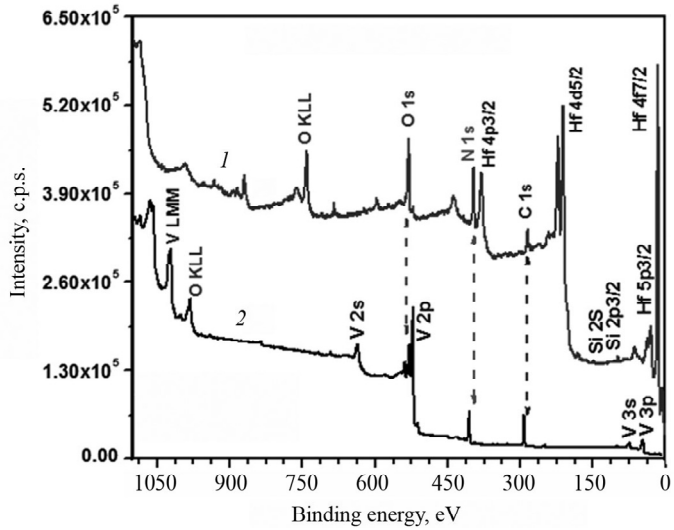


Fig. 2. XPS spectra (survey) of Hf–C–N (*1*) and V–C–N (*2*) coatings deposited on Si (100) substrates with a negative bias voltage of –50 V. The intensity of spectral signals is slightly shifted to improve observation.

### Fourier transform infrared spectroscopy (FTIR)

Fourier transform infrared spectroscopy (FTIR) analysis for Hf–C–N and V–C–N coatings deposited on Si substrates (100) under transmittance mode is shown in Fig. 4. These FTIR results show for the Hf–C–N system an absorption band centered around 500 $cm^{-1}$ and for high wave number values, a large absorption band arises around 2500 $cm^{-1}$. For the V–C–N material four absorption bands are observed, centered around 509, 683 $cm^{-1}$ and for high wave number values absorption bands arises around 1010 and 1718 $cm^{-1}$. Deconvolution of FTIR spectra by Gaussian fits was conducted to observe the intensity and position of the bands with the most significant intensity peaks (see Figs. 4, *a*, *b*). Vibration modes were found that are characteristic for metal ceramic materials. For the HfCN coating three different absorption bands were detected in a range between 500 and 1200 $cm^{-1}$ associated to Hf–C, Hf–N and Hf–C–N compounds located at 605, 793, and 1073 $cm^{-1}$, respectively [29, 30]. Moreover, around 1600, 1979, 2330, and 2786 $cm^{-1}$ wave numbers absorption bands were found, which can be associated to the contribution of the anti-symmetric stretching mode of C–O, C=N, C=C and C–H molecules, respectively [30]. For the VCN system six different absorption bands were detected in a range between 509 and 1718 $cm^{-1}$ associated to V–N, V–C–N, N–V–N, C–C, C–N, and C=C compounds located at 535, 683, 824, 1016, 1351 and 17018 $cm^{-1}$, respectively [24, 28]. The bands observed in the FTIR results can be attributed to the ternary Hf–C–N and V–C–N compounds taking into account the XRD (see Fig. 1) and of XPS (see Fig. 2) results, evidencing that N and C have reacted with hafnium and vanadium to form the ternary compounds.

### Crystallographic simulation with CaRIne crystallography 3.1 software

In order to carry out the crystal structure simulation for the HfCN and VCN coatings, the CaRIne 3.1 software was implemented. This software requires as

input parameters the elements factor occupation (stoichiometric relation) that constitutes the coatings, which is obtained experimentally from XPS analysis, the atomic radius for each element, the crystal structure, and the lattice parameter, which were extracted from the XRD analysis. Another parameter required for the crystallographic simulation is the spatial group which is obtained theoretically from the JCPDF files corresponding to the HfCN and VCN materials that show a stoichiometric composition and a similar diffraction pattern. For this specific case, reference files of HfN, HfC, VN and VC were taken as reference.

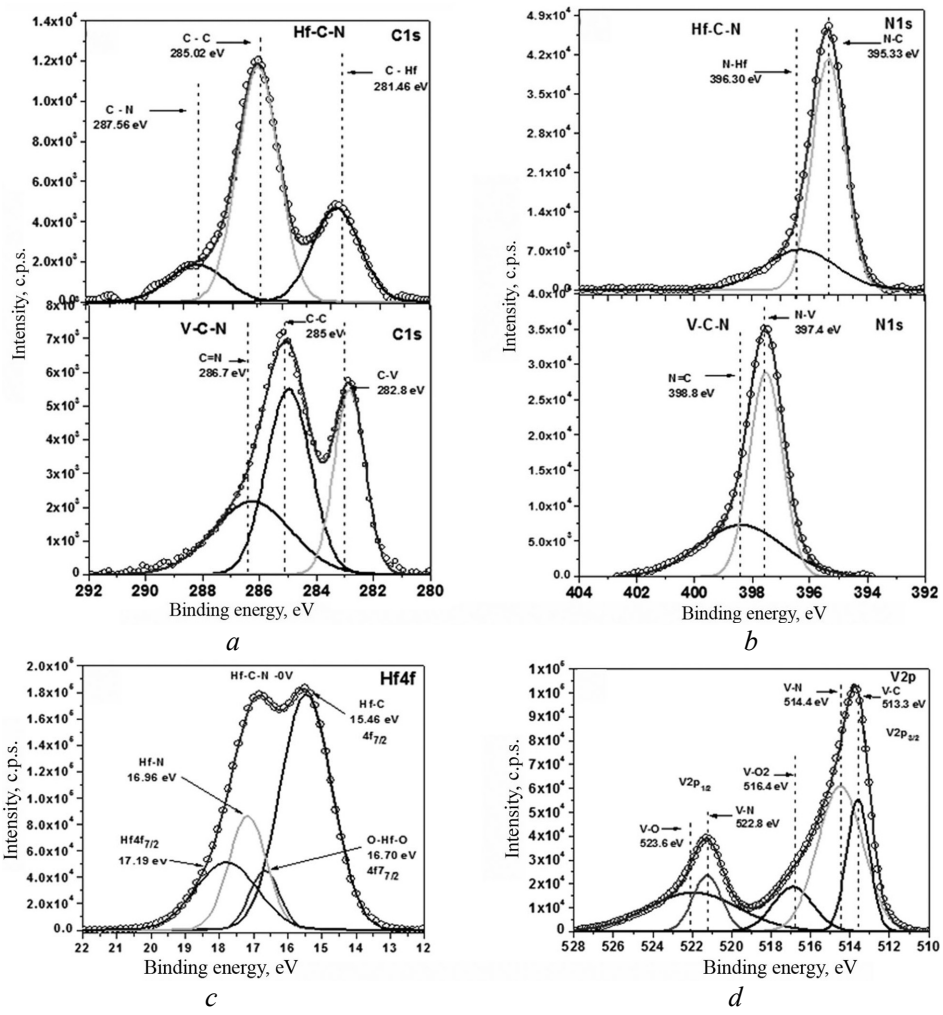


Fig. 3. High-resolution XPS spectra for Hf–C–N and V–C–N coatings: C1s signal (*a*), N1s signal (*b*), Hf4f (*c*) signal and V2p signal (*d*).

According to the above, it is intended to simulate the crystalline structures of Hf–C–N and V–C–N systems. In this sense, the occupation factor of $Hf_{57}C_{20}N_{23}$ and $V_{47}C_{21}N_{32}$ was taken from the XPS results. Continuing with another required parameter, it is necessary to extract the lattice parameter which was determinated by XRD analysis whose result was HfCN = 4.559 Å and VCN = 4.168 Å. Finally, the crystal structure resulting from the simulation for the Hf–C–N and V–C–N coatings are shown in the Figs. 5, *a*, *b* respectively. These figures respectively show the FCC crystal structure; in said structures the Hf and V atoms are located in

the positions (000) while the N and C atoms are located in the octahedral positions (1/21/21/2).

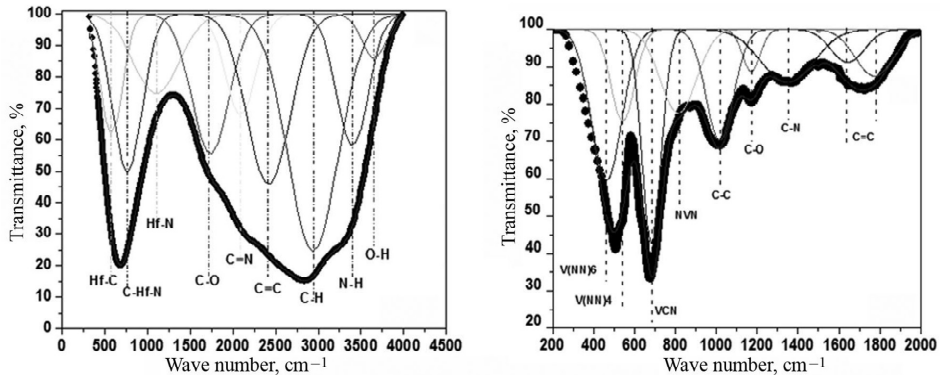


*a* *b*

Fig. 4. Deconvolution from FTIR spectra obtained for Hf–C–N (*a*) and VCN (*b*) coatings deposited on Si (100) substrates with a negative bias voltage of –50 V, showing absorption bands of different molecular interaction signals.

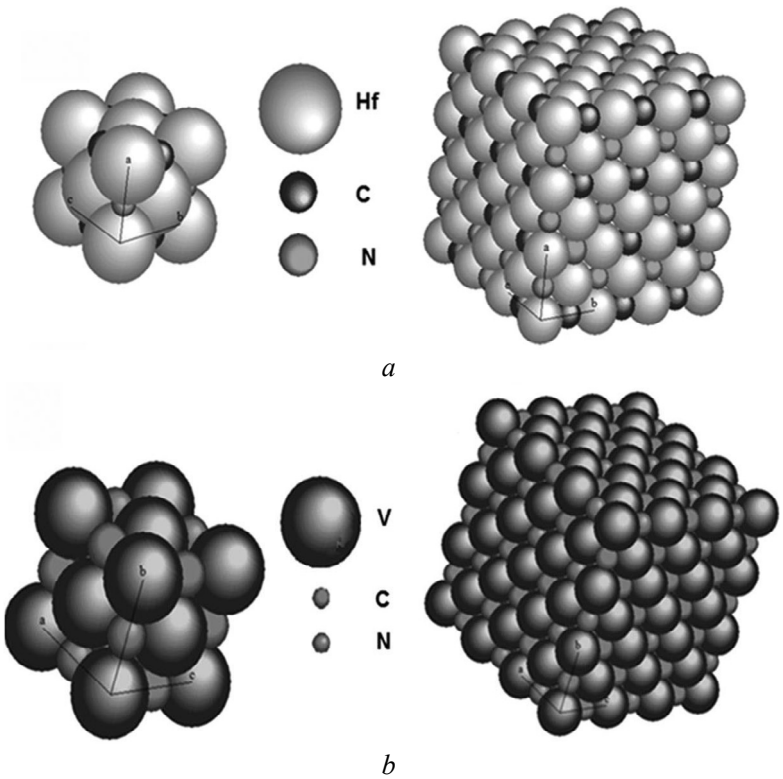


*a*

*b*

Fig. 5. Crystallographic simulation for unitary cell and crystal lattice of ternary molecule obtained by the CaRIne Crystallography 3.1 software: Hf–C–N material (*a*) and, V–C–N material (*b*).

The diffraction pattern resulting from the simulation for the Hf–C–N and V–C–N coatings are shown in the Figs. 6, *a*, *c*, and Figs. 6, *b*, *d*, respectively. In the Figs. 6, *a*, *b*, and Figs. 6, *c*, *d* it is possible to compare the XRD patterns obtained experimentally and obtained by simulation, where it can be effectively examined that

there exist a coincidence of diffraction angles in both patterns, and a coincidence with the intensities ratio of the preferential peaks. The last result is a consequence of the ternary compound's nature that presents preferential crystallographic direction (111) which is possible to attribute to the diffraction patterns simulation, and that can be attributed to the HfCN and VCN molecules where the atoms of the elements form the FCC structure type NaCl.

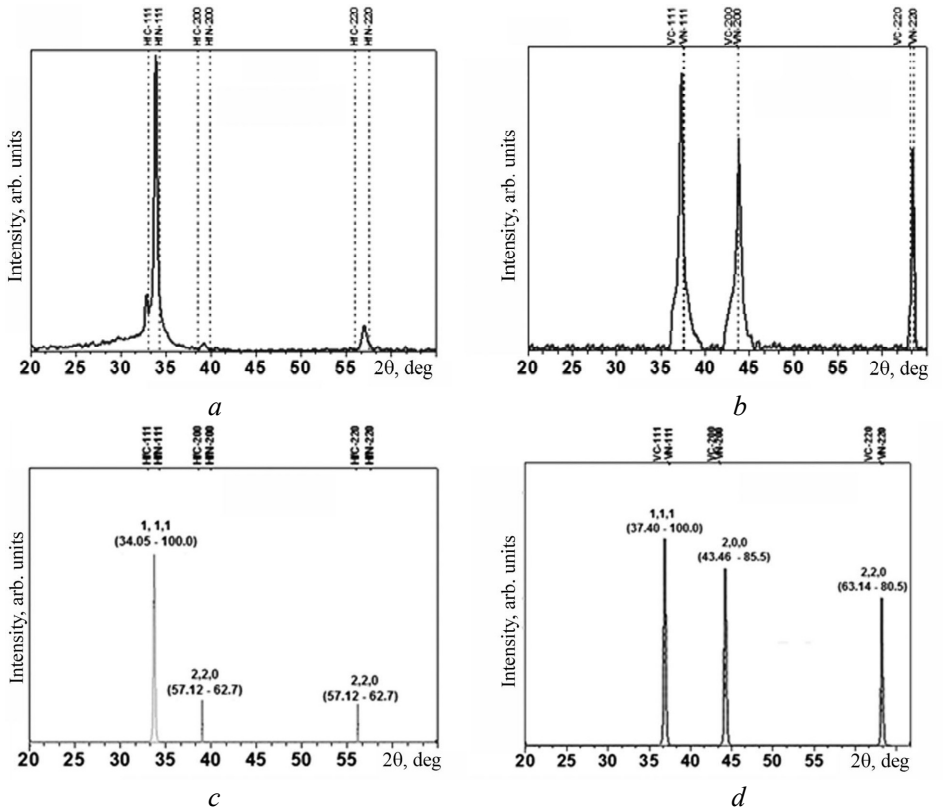


Fig. 6. Experimental (*a*, *b*) and crystallographic structures simulation (*c*, *d*) XRD patterns for ternary molecules obtained by the CaRIne Crystallography 3.1 software: Hf–C–N material (*a*, *c*) and V–C–N material (*b*, *d*).

## Atomic force microscopy (AFM)

The AFM technique was used to quantitatively analyze the surface morphology of the HfCN and VCN coatings deposited on Si substrates. In Fig. 7, *a* 50×50 μm$^2$ sample area was analyzed with a scale in Z around 7.361 nm. Two-dimensional images were obtained in no-contact mode, permitting us to determine the morphologic characteristics of the Hf–C–N and V–C–N coatings, like grain size and roughness by using an image processor (SPIP®) after the statistical analysis for each image. With this, it is possible to perceive differences in the grain size and surface roughness between the Hf–C–N and V–C–N coatings, which can be associated to densification generated by the Hf element in the Hf–C–N material. The values for the grain size were around 49 nm for VCN and 37 nm for HfCN and the values for the roughness were around 5.1 nm for VCN and 1.2 nm for HfCN so a difference of 25 % in grain size and 76 % in roughness was found (Figs. 8, *a*, *b*).

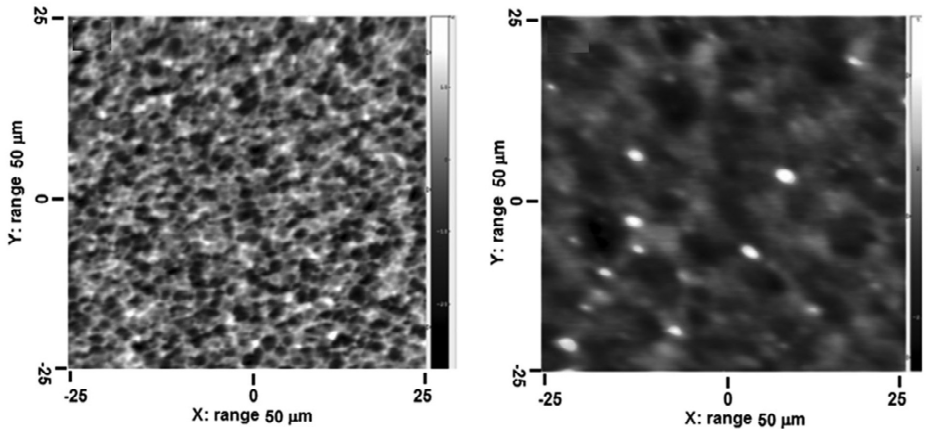


*a* *b*

Fig. 7. AFM image of coatings, showing the morphological surface with changes in surface roughness and grain size: Hf–C–N (*a*) and V–C–N (*b*).

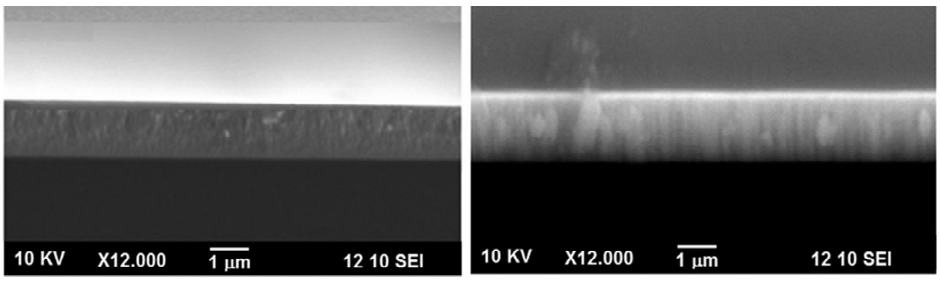


*a* *b*

Fig. 8. SEM image for coatings, showing changes in columnar growth and coatings densification: Hf–C–N (*a*) and V–C–N (*b*).

## Scanning electron microscopy (SEM)

Through scanning electron microscopy technique, a columnar growth of Hf–C–N and V–C–N coatings deposited on oriented Si (100) can be observed. Figs. 8, *a*, *b* show cross-sectional SEM images with Hf–C–N and V–C–N coating's thickness around 1.8 μm. Thus, it is possible to detect changes in the columnar growth between Hf–C–N and V–C–N coatings which can be associated to densification generated by the Hf element under increased $Ar^+$ ion impact. The columnar growth reduction and the increasing coating densification of the Hf–C–N material is related to the increased residual stress observed by XRD results (see Figs. 1 and 6) and also to the reduced grain size and roughness, as observed in AFM results (see Fig. 7).

## Nanoindentation analysis

The hardness and Young's modulus or reduced elastic modulus (*Er*) were measured for the Hf–C–N and V–C–N coatings deposited on AISI D3 substrates using the ASTM E2546–07 standard test through nanoindentation measurements [31, 32]. Figure 9 shows typical load-displacement curves for both coatings by using a standard Berkovich indenter. Hardness and elastic modulus values were obtained by using the Oliver and Pharr method [33].

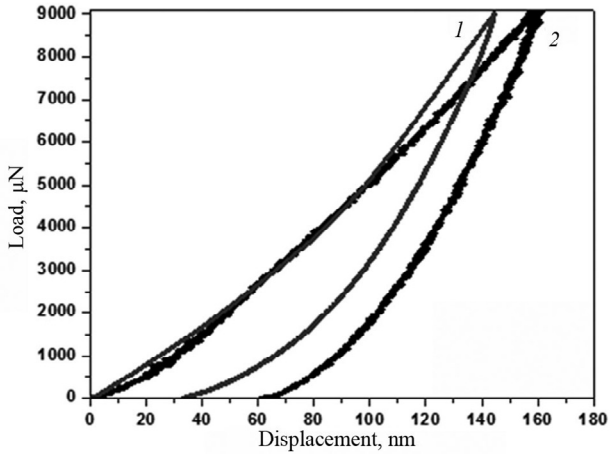

Fig. 9. Nanoindentation results for Hf–C–N (*1*) and V–C–N (*2*) coatings deposited on steel substrate showing the indentation curves (load-displacement).

From the load-displacement curves (see Fig. 9) it is possible to observe mechanical property differences (hardness) between Hf–C–N and V–C–N coatings (table). This hardness increase can be related to the increased residual stress observed via XRD (see Figs. 1 and 6) and can be corroborated with the AFM and SEM results. A change from Hf to V atoms produces a decrease in grain size and an increase in grain boundaries, thus, resulting in increased coating hardness [34].

**Mechanical and tribological properties for Hf–C–N and V–C–N coatings deposited with negative bias voltages**

| Coating | Mechanical properties | | | | Tribological properties | |
|---|---|---|---|---|---|---|
| | Hardness, GPa | Elastic modulus, GPa | Plastic deformation resistance $H^3/E^2$, GPa | Elastic recovery, % R | Friction coefficient | Critical loads, N |
| VCN | 22 | 235 | 0.194 | 60.11 | 0.49 | 21 |
| HfCN | 24 | 246 | 0.228 | 62.12 | 0.42 | 25 |

Increased hardness of these coatings is attributed to changes in the densification generated by changes in the coating composition (Hf and V), causing grain size reduction and higher coating density during deposition processes, as observed form AFM (see Figs. 6, 7) and SEM results (see Fig. 8), respectively. So, the grain boundaries can be interpreted as barriers against the free movement of dislocations in the material; therefore, a dislocation is difficult to move from one grain to another across grain boundaries due to the relative disorder of atoms in that zone, causing materials with small grains to have greater hardness. These results indicate that other mechanical properties, like elastic modulus (see table) are also highly dependent on the densification conditions.

Moreover, XRD (see Figs. 1 and 6), XPS (see Figs. 2 and 3), FTIR (see Fig. 4) and crystallographic simulation (see Fig. 5) results show that Hf–C–N and V–C–N coatings generate complex compounds, which grow with a preferential orientation in the (111) planes. Regarding the above, the literature reports that the mechanical properties of the interstitial nitrides of transition metals vary depending on the crystal orientation, usually in the (111) orientation that exhibits the hardest

structure in relation to other crystallographic directions [33, 34]. From the nanoindentation measurements (see table) it is possible to determine other mechanical properties, like plastic deformation resistance ($H^3/E^2$) and elastic recovery (% $R$). Taking into account that densification can be generated by reducing the pores and reducing the grain size, in the current research the grain size is related to the likelihood of containing a large number of dislocations, so if it is possible to reduce the grain size then this can reduce the number of dislocations; in this sense, the dislocations in the grain have restrictions (obstruction) for their free movement with the increase in the number of grain boundaries and reduction of pores.

The friction coefficient values for AISI 8620 steel substrates coated with Hf–C–N and V–C–N coatings were tested against steel balls and presented in Fig. 10. The friction coefficient curves showed two distinct stages. In the first stage (Zone I), the friction coefficient (l) began at a high level (0.53–0.56) in the first contact, respectively; this stage can be attributed to the running-in period associated with a kind of contact between the steel ball and the coating, where the formation of wear debris occurred by the cracking of roughness tips on both counterparts. This stage had a short-time period, and then the friction coefficient increased until the second stage (Zone II). This stage (zone I) is defined as the steady-state friction period and began after about 20–120 m of sliding distance (m) [36, 37]. In Zone II, from the pin-on-disk analysis picture, it was possible to observe the settling distance range (steady-state friction period) between 130 m and 400 m for each of the friction curves showing a reduction in the friction coefficient (0.42–0.49), respectively. In these results, there were no significant changes appreciated in the increase of the friction coefficient, therefore, this effect may be associated to overcome the distance of 130 m, the surfaces of the tribological pair between 100Cr6 steel pin and the Hf–C–N and V–C–N materials were normalized relative to the contact surface (Hf–C–N) which had higher Young's modulus generating a constant $Er$ and an almost invariable friction coefficient. Table shows the friction coefficient for the two carbon-nitride coatings. Tribological properties of the carbon nitride coatings (Hf–C–N and V–C–N) are provided in Fig. 10 for comparison in relation to single layer systems. These tribological results show the reduction of the friction coefficient when the transition metal was changed. In this regard, the friction coefficient value presented a decrease of approximately 14 % of the friction coefficient between Hf–C–N and V–C–N coatings.

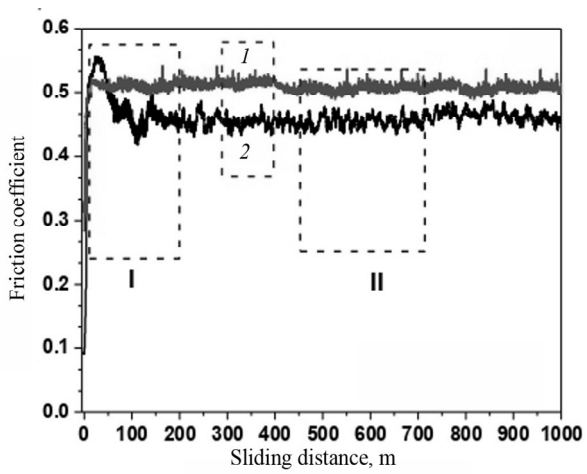


Fig. 10. Friction coefficient as a function of sliding distance for 8620 steel substrates coated with V–C–N (*1*) and Hf–C–N (*2*) coatings.

In agreement with the model presented by Archard [38], when the surface coating has low roughness and high hardness, the friction coefficient will tend to decrease and will be stable for long sliding distances, specifically if the counterpart of the test is softer than the coating.

Although hardness has long been regarded as a primary material property that defines wear resistance, strong evidences suggest that the elastic modulus can also have an important influence on the wear behavior. Therefore, it is possible to observe that the elastic strain to failure, which is related to $H/Er$ (see table), affects the tribological behavior of the Hf–C–N and V–C–N systems, which provides superior wear resistance when the coatings are deposited on the substrate materials for mechanical applications [39]. Consequently, this behavior suggests that improving plastic deformation resistance ($H^3/Er^2$) when the negative bias voltage is increased, exerts more wear resistance due to enhanced mechanical properties (see table) associated with the changes in the internal stress (previously observed in XRD results). Thus, it was possible to generate a reduction in the friction coefficient (see table).

**Adherence analysis by using a critical load criterion (Adhesion Behavior)**

The scratch test was used to characterize the coating adherence strength. The adhesion properties of HfCN and VCN coatings can be characterized by the following two terms: $L_{C1}$, the lower critical load, which is defined as the load where cracks first occurred (cohesive failure); and $L_{C2}$, the upper critical load, which is the load where the first delaminating at the edge of the scratch track occurred (adhesive failure) [39]. The values of critical load ($L_{C1}$ and $L_{C2}$) for the different coatings are shown in Fig. 11. The $L_{C1}$ for the different coatings was shown in the range of 13–18 N, in which the lowest value was attributed to the hard coatings deposited with V element (V–C–N) and the highest value was attributed to the ternary system growth with Hf element (HfCN).

In this sense, the critical loads in adhesive failure ($L_{C2}$) values for the two ternary coatings are summarized in (see table), from 21 to 25 N.

The Fig. 11 clearly shows that the adhesion properties of the metal ceramic coatings increase when the metal composition is changed from V to Hf. Due to the quantitative adhesion measurements between the layers and substrates, this process is complex even for single layer coatings.

In the tribological mechanism, the densification and grain size reduction (see Figs. 7 and table) serves as a crack tip deflector that changes the direction of the initial crack when it penetrates deep into the coating, and strengthens the coating's performance. Moreover, by decreasing the grain size, the dislocations among the grain boundaries find a major impediment to move; therefore, those dislocations will require higher critical shear stress to travel and spread throughout the coating and allow the delamination of the Hf–C–N and V–C–N coatings. This effect means that carbon nitride coatings can fail in a fragile manner [40, 41] because these coatings are homogeneous systems. In consequence, ternary single layers such as those studied in the current work can enhance the resistance of coatings against crack propagation in relation to the mechanical property evolution presented by the enhanced hardness and elastic modulus (see table) with higher elastic recovery (% $R$) (see table), preserving the integrity of the coatings under punctual (static) and dynamic loads [42, 43]. Therefore, the tribological results are associated to the physical properties observed in XPS, FTIR and AFM results.

## CONCLUSIONS

From XRD results it was possible to determine the (111) preferential orientation FCC and the lattice parameter of the carbon nitride coatings, finding a strong

relationship between lattice parameter and changes in the chemical composition when the metallic elements were changed from Hf to V to obtain the Hf–C–N and V–C–N materials respectively. Via XPS, FTIR and crystallography simulation, it was possible to observe the formation of a complex compound based on ternary Hf–C–N and V–C–N materials, given that the Hf–C–N and V–C–N systems present absorption bands and binding energies corresponding to metal-ceramic systems.

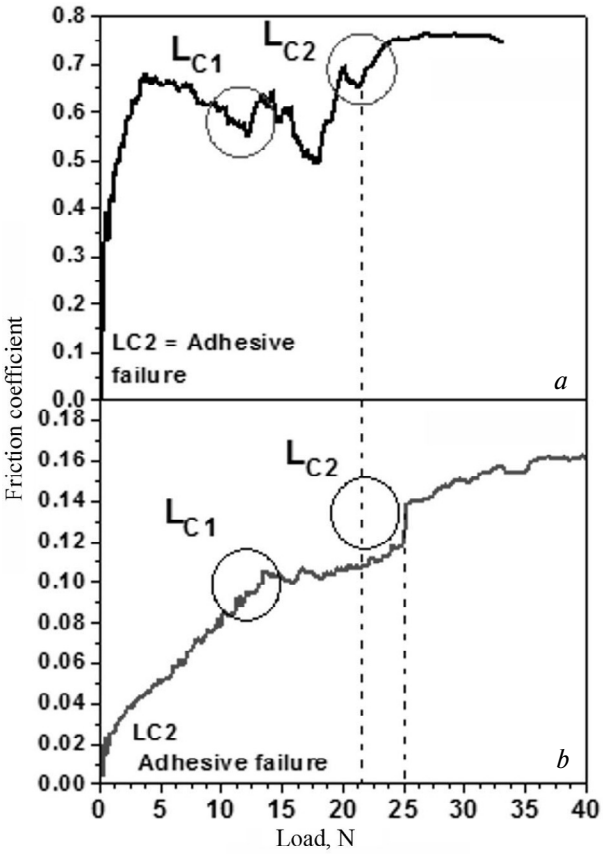


Fig. 11. Tribological results for Hf–C–N (*1*) and V–C–N (*2*) coatings deposited on AISI 8620 steel, showing the cohesive failure ($L_{C1}$) and adhesion failure ($L_{C2}$): friction coefficient curves vs. applied load (*a*) and critical loads for two different ternary coatings (*b*).

The Hf–C–N coating exhibits the highest hardness and elastic modulus in relation to V–C–N coating, showing an increase of 8 % in hardness and 4 % in elastic modulus. These results could be associated to the Hf contribution that reduced grain size and induced densification that generated a large number of interfaces which blocks the free movement of dislocations.

The lowest friction coefficient and high critical load in the ternary coatings was found when Hf atoms were introduced in the carbon nitride system instead of V. Observing thus an enhancement of the tribological properties by a 14 % reduction of the friction coefficient in the Hf–C–N coating when both coatings were compared with the same steel substrate; therefore, a lower critical load for adhesive failure was obtained in the V–C–N coating.

The lowest critical load in the coatings was found when Hf–C–N was deposited on AISI 8620 steel, observing thus an enhancement of the tribological properties

($L_{C2}$) by a 16 % increase in load resistance for the Hf–C–N coating in relation to the V–C–N coating.


## ACKNOWLEDGMENTS

This research was supported by "Vicerrectoría de Investigaciones de la Universidad Militar Nueva Granada" project number ING-2992, validity 2019. CIC biomaGUNE, San Sebastian, Spain, and the Excellence Center for Novel Materials (CENM) at Universidad del Valle in Cali, Colombia.



*Покриття Hf–C–N та V–C–N наносили на кремнієві (100) і сталеві (AISI 8620) підкладки реактивним магнетронним розпиленням з мішеней гафнію, ванадію та вуглецю в реакційній атмосфері азоту з негативною напругою зміщення –50 В. Вплив елементів Hf та V на кристалічну структуру, хімічний склад і механічні властивості спостерігали за допомогою рентгенівської дифракції, рентгенівської фотоелектронної спектроскопії, інфрачервоної спектроскопії з перетворенням Фур'є, комп'ютерного моделювання, атомно-силової мікроскопії, скануючої електронної мікроскопії, наноіндентування, прикріплення на диску і скрэтч-теста. Результати показали, що зразки мали постійне стехіометричне співвідношення, демонструючи структурні характеристики, дуже схожі на характеристики структур, що одержані комп'ютерним моделюванням. Зміна механічних властивостей заміщенням елемента Hf на V може збільшити твердість від 22 до 24 ГПа і модуль пружності з 235 до 246 ГПа. Для трибологічних властивостей було виявлено зміни для коефіцієнта тертя від 0,49 до 0,42 і для критичного навантаження від 21 до 25 Н. Тож вплив умов осадження на структуру та властивості покриттів було пов'язано з відмінностями у вмісті гафнію й ванадію в потрійних покриттях. Тому покриття Hf–C–N та V–C–N можуть використовуватися у майбутньому як матеріали твердого покриття.*



***Ключові слова**: магнетронне розпилення, карбо-нітриди металів, HfCN, VCN, механічні властивості.*



*Покрытия Hf–C–N и V–C–N были нанесены на кремниевые (100) и стальные AISI 8620 подложки реактивным магнетронным распылением от мишеней из гафния, ванадия и углерода в атмосфере химически активного азота с отрицательным напряжением смещения –50 В. Влияние элементов Hf и V на кристаллическую структуру, химический состав и механические свойства наблюдали с помощью рентгеновской дифракции, рентгеновской фотоэлектронной спектроскопии, инфракрасной спектроскопии с Фурье-преобразованием, компьютерного моделирования, атомно-силовой микроскопии, сканирующей электронной микроскопии, наноиндентирования, метода закрепления на диске и скрэтч-теста. Результаты показали, что образцы имели постоянное стехиометрическое соотношение, демонстрируя структурные характеристики, очень похожие на характеристика моделируемых структур. Изменения механических свойств путем замены элемента Hf на V могут повысить твердость с 22 до 24 ГПа и модуль упругости с 235 до 246 ГПа. Для трибологических свойств были выявлены изменения коэффициента трения от 0,49 до 0,42 и критической нагрузки от 21 до 25 Н. Таким образом, влияние условий осаждения на структуру и свойства покрытий было связано с различиями в содержании гафния и ванадия в тройных покрытиях. Поэтому покрытия Hf–C–N и V–C–N могут использоваться в качестве будущих материалов для твердого покрытия.*



***Ключевые** слова: магнетронное распыление, карбо-нитриды металлов, HfCN, VCN, механические свойства.*



1. Bakoglidis K.D., Schmidt S., Greczynski G., Hultman L. Improved adhesion of carbon nitride coatings on steel substrates using metal HiPIMS pretreatments. *Surf. Coat. Technol*. 2016. Vol. 302. P. 454–462.
2. Cheng Y.H., Browne T., Heckerman B. TiCN coatings deposited by large area filtered arc deposition technique. *J. Vacuum Sci. Technol. A*. 2010. Vol. 28. P. 431.
3. Hovsepian P.Eh. Ehiasarian A.P., Petrov I. Structure evolution and properties of TiAlCN/VCN coatings deposited by reactive HIPIMS. *Surf. Coat. Technol*. 2014. Vol. 257. P. 38–47.

4. Tokoroyama T., Hattori T., Umehara N., Kousaka H., Manabe K., Kishi M., Fuwa Y. Ultra-low friction properties of carbon nitride tantalum coatings in the atmosphere. *Tribology Int.* 2016. Vol. 103. P. 388–393.
5. Serro A.P., Completo C., Colaço R., dos Santos F., Lobato da Silva C., Cabral J.M.S., Araújo H., Pires E., Saramago B. A comparative study of titanium nitrides, TiN, TiNbN and TiCN, as coatings for biomedical applications. *Surf. Coat. Technol*. 2009. Vol. 203. P. 3701–3707.
6. Lu X.J., Xiang Z.D. Formation of chromium nitride coatings on carbon steels by pack cementation process. *Surf. Coat. Technol*. 2017. Vol. 309. P. 994–1000.
7. Piedrahita W.F., Aperador W., Caicedo J.C., Prieto P. Evolution of physical properties in hafnium carbonitride thin films. *J. Alloys Comp*. 2017. Vol. 690. P. 485–496.
8. Caicedo J.C., Aperador W., Mozafari M., Tirado L. Evidence of electrochemical resistance on ternary V–C–N layers. *Silicon.* 2018. Vol. 10. P. 1–9.
9. Maugis P., Goune M. *Acta Mater.*. 2005. Vol. 53. P. 3359–3367.
10. Hovsepian P.Eh., Ehiasarian A.P., Petrov I. *Surf. Coat. Technol*. 2014. Vol. 257. 38–47.
11. Heo. S.Y, Shin J.H., Kim D.-I., Oh J.Y., Zhang S.H., Kim K.H. Microstructure and mechanical properties of Cr–V–C–N films. *Surf. Eng*. 2015. Vol. 31. P. 513–518.
12. Yun J.S., Hong Y.S., Kim K. H. Characteristics of ternary Cr–O–N coatings synthesized by using an arc ion plating technique. *J. Korean Phys. Society*. 2010. Vol. 57. P. 103–110.
13. Caicedo J.C., Amaya C., Cabrera G., Esteve J., Aperador W., Gómez M.E., Prieto P. Corrosion surface protection by using titanium carbon nitride/titanium-niobium carbon nitride multilayered system. *Thin Solid Films*. 2011. Vol. 519. P. 6362–6368.
14. Levi G., Kaplan W.D., Bamberger M. Structure refinement of titanium carbonitride (TiCN). *Mater. Lett*. 1998. Vol. 35. P. 344–350.
15. Caicedo J.C., Zambrano G., Aperador W., Escobar-Alarcon L., Camps E. Mechanical and electrochemical characterization of vanadium nitride (VN) thin films..*Appl. Surf. Sci.* 2011. Vol. 258, iss. 1. P. 312–320.
16. Romero J., Esteve J., Lousa A. Surf. Period dependence of hardness and microstructure on nanometric Cr/CrN multilayers. *Coat. Technol*. 2004. Vol. 188–189. P. 338–343.
17. Baba Y., Sasaki T.A., Takano I. Preparation of nitride films by Ar+-ion bombardment of metals in nitrogen atmosphere. *J. Vac. Sci. Technol. A*. 1988. Vol. 6, iss. 5, art. 2945.
18. Ramqvist L., Hamrin K., Johansson G., Fahlman A., Nordling C. Charge transfer in transition metal carbides and related compounds studied by ESCA. *J. Phys. Chem. Solids.* 1969. Vol. 30. P. 1835–1847.
19. Beamson G., Briggs D. High resolution XPS of organic polymers: the scienta ESCA300 database. Chichester: John Wiley, 1992. 295 p.
20. Ech-Chamikh E., Essafti A., Ijdiyaou Y., Azizan M. XPS Study of amorphous carbon nitride (a-C:N) thin films deposited by reactive rf sputtering. *Sol. Energy Mater. Sol. Cells.* 2006. Vol. 90. P. 1420–1423.
21. Han B., Yu L., Hevesi K., Gensterblum G., Rudolf P., Pireaux J.-J. Electronic transitions and excitations in solid C70 studied by EELS and XPS C 1s satellite structures. *Phys. Rev. B.* 1995. Vol. 51, art. 7179.
22. Tucker M.D., Czigány Z., Broitman E., Näslund L.-Å., Hultman L., Rosen J. Filtered pulsed cathodic arc deposition of fullerene-like carbon and carbon nitride films. *J. Appl. Phys*. 2014. Vol. 115, art. 144312.
23. Steiner P., Hüfner S. Heat of mixing in $HfC_xN_{1-x}$ compounds from XPS core level binding energy shifts. *Solid State Commun*. 1982. Vol. 44, no. 8. P. 1305–1307.
24. Grigore E., Ruset C., Luculescu C. The Structure and properties of VN–VCN–VC coatings deposited by a high energy ion assisted magnetron sputtering method. *Surf. Coat. Technol*. 2011. Vol. 205. P. 29–32.
25. Li J., Liu X., Cao C., Guo J., Pan Z. Silica-gel supported V complexes: preparation, characterization and catalytic oxidative desulfurization. *Chinese J. Chem. Eng*. 2013. Vol. 21, no. 8. P. 860–866.
26. Bacal M., Perrière J., Tanguy M., Vesselovzorov A., Maslakov K., Dementjev A. Study of carbon nitride films deposited using a hall-type ion source. *J. Phys. D. Appl. Phys.* 2000. Vol. 33, no. 19. P. 2373–2378.
27. Franz R., Neidhardt J., Sartory B., Tessadri R., Mitterer C. Micro- and bonding structure of arc-evaporated AlCrVN hard coatings. *Thin Solid Films*. 2008. Vol. 516, no. 18. P. 6151–6157.

28. Yan. X., Xu T., Chen G., Yang S., Liu H., Xue Q. Preparation and characterization of electrochemically deposited carbon nitride films on silicon substrate. *J. Phys. D: Appl. Phys*. 2004. Vol. 37. P. 1–7.
29. Sarma D.D., Rao C.N.R. XPES studies of oxides of second-and third-row transition metals including rare earths *J. Electron Spectrosc. Relat. Phenom*. 1980. Vol. 20, iss. 1. P. 25–45.
30. Volland W. Organic Compound Identification Using Infrared Spectroscopy. Bellevue Community College, 1999.
31. Standard Practice for Instrumented Indentation Testing. ASTM E2546–07.
32. Escobar C., Villarreal M., Caicedo J.C., Aperador W., Prieto P. mechanical properties of steel surfaces coated with HfN/VN superlattices. *J. Mater. Eng. Perform.* 2014. Vol. 23. P. 3963–3974.
33. Oliver W., Pharr G. *J.* An improved technique for determining hardness and elastic modulus using load and displacement sensing indentation experiments. *Mater. Res*. 1992. Vol. 7, iss. 6. P. 1564–1583.
34. Tjong S.C., Chen H. Nanocrystalline materials and coatings. *Mater. Sci. Eng. R*. 2004. Vol. 45, iss. 1–2. P. 1–88.
35. Hajek V., Rusnak K., Vlcek J., Martinu L., Hawthorne H.M. Tribological study of $CN_x$ films prepared by reactive d.c. magnetron sputtering. *Wear*. 1997. Vol. 213, no. 1–2. P. 80–86.
36. Martínez E., Romero J., Lousa A., Esteve J. *Appl. Phys. A*. 2003. Vol. 77, no. 3–4. P. 419–426.
37. Holleck H., Lahres M., Woll P. Multilayer coatings–influence of fabrication parameters on constitution and properties. *Surf. Coat. Technol*. 1990. Vol. 41. P. 179–190.
38. Archard J.F. Contact and rubbing of flat surfaces. *J. Appl. Phys*. 1953. Vol. 24, no. 8. P. 981–988.
39. Leyland A., Matthews A. On the significance of the *H*/*E* ratio in wear control: A nanocomposite coating approach to optimised tribological behaviour. *Wear*. 2000. Vol. 246. P. 1–11.
40. Veprek S., Reiprich S.A. Concept for the design of novel superhard coatings. Thin *Solid Films*. 1995. Vol. 268. P. 64–71.
41. Podgornik B., Hogmark S., Sandberg O., Leskovsek V. Wear resistance and anti-sticking properties of duplex treated forming tool steel. *Wear*. 2003. Vol. 254, iss. 11. P. 1113–1121.
42. Holmberg K., Ronkainen H., Matthews A. Tribology of thin coatings. *Ceram. Int.* 2000. Vol. 26, iss. 7. P. 787–795.
43. Escobar C., Villarreal M., Caicedo J.C., Esteve J., Prieto P. Mechanical and tribological behavior of VN and HfN films deposited via reactive magnetron sputtering. *Surface Rev. Lett*. 2013. Vol. 20, no. 3–4, art. 1350040.

Received 21.11.18
Revised 01.04.19
Accepted 05.04.19